Progressive failure of slopes with sensitive clay layers

Rupture progressive de pentes comportant des couches d'argile sensible

Dey R., Hawlader B.
Memorial University of Newfoundland, St. John's, Canada.

Phillips R.
C-CORE, St. John's, Canada.

Soga K.
University of Cambridge, Cambridge, UK.

ABSTRACT: Progressive failure of slopes can trigger large scale landslides. The presence of sensitive clay layers is one of the main reasons for progressive failure of a slope. The whole soil mass involved in a potential landslide might be of sensitive clay, while in some cases there exist only thin layers of sensitive clay interbedded with relatively strong soils. The movement of a slope might be initiated due to the presence of a weak soil layer, where the shear stress is increased or soil strength is reduced by various triggering factors. Once the failure/movement is initiated in a small zone, the imbalanced force is transferred to the surrounding soil in which slip surface might propagate in the form of a shear band through the sensitive clay layer even though the sensitive clay layer is relatively thin. The propagation of shear band in sensitive clay is also associated with post-peak strain softening behaviour of soil. In this study, upward progressive failure due to river bank erosion has been modelled using nonlinear post-peak strain softening behaviour. It is shown that the pattern of propagation of shear band varies with soil type and slope geometry.

RÉSUMÉ : La rupture progressive de pentes peut déclencher des glissements de terrain de grande envergure. La présence de couches d'argile sensible est l'une des principales raisons de la rupture progressive d'une pente. La masse de sol impliquée dans un glissement de terrain potentiel pourrait être totalement constituée d'argile sensible, alors que dans certains cas, il existe seulement des couches minces d'argile sensible intercalées entre des sols relativement résistants. Le mouvement d'une pente peut être initié en raison de la présence d'une couche de sol peu résistant, dans laquelle le taux de cisaillement augmente ou sa résistance diminue en raison de divers facteurs de déclenchement. Lorsque la rupture / le mouvement sont initiés dans une petite zone, le déséquilibre de force se développe vers le sol environnant, dans lequel la surface de glissement peut se propager sous forme d'une bande de cisaillement à travers la couche d'argile sensible, même si la couche d'argile sensible est relativement mince. La propagation des bandes de cisaillement dans l'argile sensible est également associée au ramollissement post-pic du comportement du sol. Dans cette étude, la rupture progressive amont due à l'érosion des berges a été modélisée par le ramollissement non-linéaire post-pic du comportement. Il est montré que le faciès de propagation des bandes de cisaillement varie en fonction du type de sol et de la géométrie de la pente.

KEYWORDS: Sensitive clay, progressive failure, spread, shear band propagation, strain softening.

1. INTRODUCTION

Large landslides in soft sensitive clays are common in Eastern Canada and Scandinavia. Most of the onshore slides which occurred in soft sensitive clay have been reported as progressive in nature (Bernander 2000, Locat et al. 2008, Quinn 2009, Locat et al. 2011). The presence of strain-softening clay layers is one of the main reasons for progressive failure of a slope.These slides could be in the form of multiple retrogressive, translational progressive or spreads (Tavenas 1984, Karlsrud et al. 1984). Failure might be initiated in a fully stable and/or marginally stable slope depending on the nature of triggering factors. Failure could propagate either in upward or downward direction and the movement of the slope might be initiated due to the presence of a weak soil layer, where the shear stress is increased or soil strength is reduced by various triggering factors. Large landslides in sensitive clays classified as spread (Cruden and Varnes 1996) might be triggered by erosion near the toe of the river bank slope (Quinn et al. 2007, Locat et al. 2008). Numerous spread failures such as Sköttorp landslide in Sweden (Odenstad 1951) and the landslides occurred in Quebec including 1989 Saint-Liguori landslide (Grondin and Demers 1996), Saint-Ambroise-de-Kildare landslide (Carson 1979), Saint-Barnabé-Nord slide (Locat et al. 2008) have been reported to be triggered by erosion at the toe of the slope (Bernander 2000, Locat et al. 2008, Quinn et al. 2007, Locat et al. 2011), although it is very difficult to identify the true disturbing agents which caused these spread failures.

Progressive failure might occur in drained as well as undrained conditions. Bjerrum (1967) explained upward progressive failure initiation in an intact slope containing overconsolidated plastic clays and clay shales and considered the failure as drained. Sensitive clays from Eastern Canada and Scandinavia show strain softening behavior under undrained loading which has been considered as one of the main reasons for developing progressive failure (Bernander 2000, Locat et al 2008, Quinn 2009, Locat et al 2011). Hence undrained condition is considered in this study for analyzing spread failure.

During Ormen Lange field development, numerical simulations have been carried out by Norwegian Geotechnical Institute (NGI) using PLAXIS software to analyze the potential of retrogressive sliding due to strain softening effect in mild clay slopes (NGI 2001). Anderson and Jostad (2007) conducted numerical analyses of progressive failure of slope by modeling the shear band as an interface element using the NGI finite element (FE) code BIFURC. Quinn (2009) also demonstrates the use of linear elastic fracture mechanics concept in progressive failure of slopes.

This paper describes a numerical technique which can be used to analyze the spread or upward progressive failure of a slope typically occurs in river banks due to toe erosion.

2. PROBLEM DEFINITION

The geometry of the slope modeled in this study is shown in Fig. 1. The river bank has a slope of 30° to the horizontal. A thick crust of overconsolidated clay near the face of the slope and below the ground surface is assumed. For simplicity the

groundwater table is assumed at the crest of the slope and the river is full. A block of soil near the toe of the slope shown by the hatched zone is removed, which could be caused by erosion or by excavation in the field. This block will be referred as "excavated/eroded soil block." It is also assumed that the erosion or excavation is occurred relatively fast such that the deformation/failure of remaining soil is in undrained condition.

Three cases are simulated in this study. In Case-I, the ground surface is horizontal and there is a 15 m thick layer of sensitive clay below the 5 m crust. The Case-II is same as Case-I but the ground surface is inclined upward at 4°. Sometimes in the field there may not be a thick sensitive clay layer. To investigate the effect of thickness of the sensitive clay layer, in Case-III only 1.0 m thick sensitive clay layer parallel to the horizontal ground surface from the toe of the slope is assumed. The soil above this layer has the same geotechnical properties of the crust used in Cases I & II. In all three cases, the base layer below the toe of the slope is very stiff and therefore the failure is occurred in the soil above the base layer. The length of the soil domain in the present FE model is 500 m and therefore no significant effects on the results are expected from the right boundary.

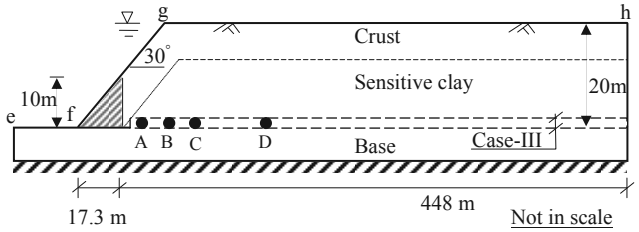

Figure 1. Geometry of the slope used in numerical analysis

3. FINITE ELEMENT MODELING

3.1 Numerical technique

ABAQUS 6.10 EF-1 is used in this study. The progressive slope failure is fundamentally a large deformation problem as very large plastic shear strain is developed in a thin layer of soil through which the failure of the slope is occurred. Conventional finite element techniques developed in Lagrangian framework cannot model such large strain problems because significant mesh distortion occurs. In order to overcome these issues, Coupled Eulerian-Lagrangian (CEL) technique currently available in ABAQUS FE software is used. The finite element model consists of three parts: (i) soil, (ii) excavated/eroded soil block, and (iii) void space to accommodate displaced soil mass. The soil is modeled as Eulerian material using EC3D8R elements, which are 8-noded linear brick, multi-material, reduced integration with hourglass control elements. In ABAQUS CEL, the Eulerian material (soil) can flow through the fixed mesh. Therefore, there is no numerical issue of mesh distortion or mesh tangling even at large strain in the zone around the failure plane.

The excavated/eroded soil block is modeled in Lagrangian framework as a rigid body, which makes the model computationally efficient. A void space is created above the model shown in Fig. 1 using the "volume fraction" tool. Soil and void spaces are created in Eulerian domain using Eulerian Volume Fraction (EVF). For void space EVF is zero (i.e. no soil). On the other hand, EVF is unity in clay layers shown in Fig. 1, which means these elements are filled with Eulerian material (soil).

Zero velocity boundary conditions are applied at all faces of the Eulerian domain (Fig.1) to make sure that Eulerian materials are within the domain and cannot move outside. That means, the bottom of the model shown in Fig. 1 is restrained from any movement, while all the vertical faces are restrained from any lateral movement. No boundary condition is applied at the soil-void interface (efgh in Fig. 1) so that the soil can move into the void space when displaced.

Only a three-dimensional model can be generated in ABAQUS CEL. In the present study the model is only one element thick, which represents the plane strain condition.

The numerical analysis consists of two steps of loading. In the first step geostatic load is applied to bring the soil in in-situ condition. Note that under geostatic step the slope is stable with some shear stress especially near the river bank. In the second step, the rigid block of excavated/eroded soil is moved horizontally 2 m to the left using displacement boundary condition.

3.2 Soil parameters

Table 1 shows the geotechnical parameters used in this study. The crust has an average undrained shear strength of 60 kPa, and a modulus of elasticity of 10 MPa (=167s_u). The soil in the base layer is assumed to be very strong and s_u=250 kPa and E_u=100 MPa is used.

Table 1. Parameters for finite element modelling.

Crust	
Undrained modulus of elasticity, E_u (kPa)	10,000
Undrained shear strength, s_u (kPa)	60
Submerged unit weight of soil, ©2 (kN/m^3)	9.0
Poisson's ratio, ⌇$_u$	0.495
Sensitive clay	
Undrained modulus of elasticity, E_u (kPa)	7,500
Poisson's ratio, ⌇$_u$	0.495
Peak undrained shear strength, s_{up} (kPa)	50
Residual undrained shear strength, s_{ur} (kPa)	10
Submerged unit weight of soil, ©2 (kN/m^3)	8.0
Plastic shear strain for 95% degradation of soil strength, γ^p_{95} (%)	33

Proper modeling of stress-strain behavior of sensitive clay layer is the key component of progressive failure analyses in sensitive clays. When sensitive clay is subjected to undrained loading it shows post-peak softening behavior. Various authors (e.g. Tavenas et al. 1983, Quinn 2009) showed that the post-peak softening behavior is related to post-peak displacement or plastic shear strain. The following exponential relationship of shear strength degradation as a function of plastic shear strain is used in the present study.

$$s_u=[1+(S_t-1)\exp(-3\delta/\delta_{95})]s_{ur} \quad (1)$$

where s_u is the strain-softened undrained shear strength at δ; S_t is sensitivity of the soil; ™=™$_{total}$-™$_p$ where ™$_p$ is the displacement required to attain the peak undrained shear strength (s_{up}); and δ_{95} is the value of δ at which the undrained shear strength of the soil is reduced by 95% of (s_{up}-s_{ur}). Equation 1 is a modified form of strength degradation equation proposed by Einav and Randolph (2005) and was used by the authors (Dey et al. 2012) to model submarine landslides. If the thickness of shear band (t) is known, the corresponding plastic shear strain (γ^p) can be calculated as, $\gamma^p=\delta/t$ assuming simple shear condition. Therefore, Eq.1 in terms of γ^p can be written as

$$s_u=[1+(S_t-1)\exp(-3\gamma^p/\gamma^p_{95})]s_{ur} \quad (2)$$

where γ^p_{95} is the value of γ^p at 95% strength reduction (i.e. $\gamma^p_{95}=\delta_{95}/t$). Note that, it is very difficult to determine the thickness of the shear band in the field. Similar to some previous studies (e.g. Quinn 2009) t=0.375 m is used which is same as the mesh height used in the present FE analysis. In ABAQUS the degradation of shear strength of sensitive clay is varied as a function of plastic strain. The parameters used to

model the sensitive clay using Eq. 2 are also shown in Table 1. These parameters are estimated based on the laboratory tests conducted on sensitive clays (e.g. Tavenas et al., 1983) and the interpretation of test data and constitutive model development by other researchers (e.g. Bernander 2000, Leroueil 2001, Locat et al. 2008, Quinn 2009, Locat et al. 2011).

4. FINITE ELEMENT RESULTS

4.1 Propagation of shear band

Figure 2 shows the variation of equivalent plastic shear strain for three cases. In Cases-I & II the shear band initially propagates horizontally and then curved upward resulting in global failure. The failed soil mass follows the excavated/eroded soil block. Figures 2(a) & 2(b) show the equivalent plastic shear strain when the plastic shear strain in the entire failure plane is greater than γ^p_{95}. Global failure does not occur in Case-III (Fig. 2c). There is an approximately 1.4 m gap between the vertical face of the block and soil mass at the right. The shear band propagates horizontally and finally ended at certain length. Figure 2(c) also shows the plastic shear strain when the shear band propagation is ended. Whether the shear

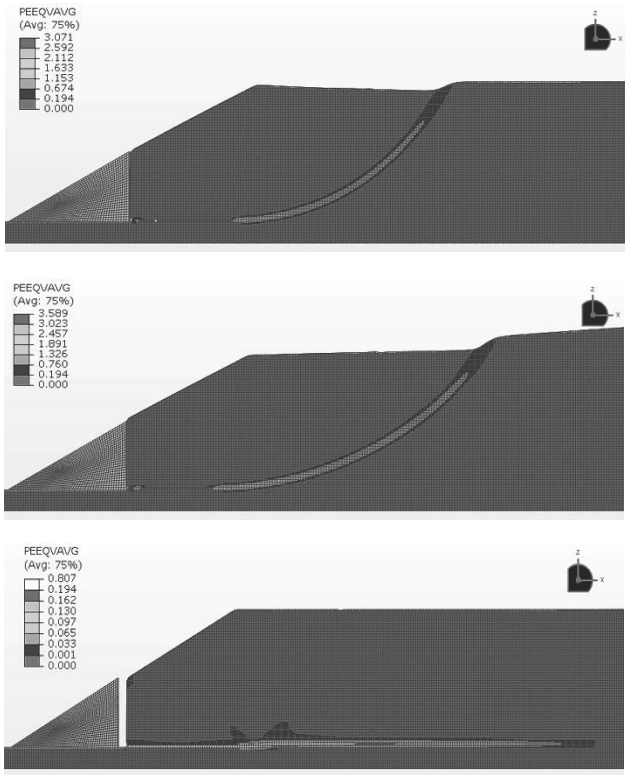

Figure 2. Developed equivalent plastic strain in the softening layer in case I, II and III respectively

band will propagate upward and cause the global failure or not, depends on the shear strength of the upper soil layer and mobilized shear strength along the shear band. For the soil properties and geometry used in the present study the failure pattern is almost same for Cases-I and II. However, the released energy from the excavated/eroded soil block is not sufficient to move the shear band upward in Case-III to cause the failure of the slope.

The equivalent plastic shear strain, denoted by the symbol PEEQVAVG in Fig. 2, is related to γ^p as PEEQVAVG= γ^p/ . According to Eq. (2), when $\gamma^p \varepsilon \gamma^p_{95}$ (=33%), that means PEEQVAVG=0.194, the undrained shear strength is less than 12 kPa (=50-0.95(50-10)). Figure 2(c) shows that the equivalent plastic shear strain greater than 0.194 is developed in the shear band only near the vertical face of excavated/eroded block in Case-III. However, the equivalent plastic shear strain greater than 0.194 is developed in the entire length of the failure plane in Case-I & Case-II. Therefore, the failure of the slope is occurred in both cases at residual shear strength on the failure plane as large strain is developed.

4.2 Shear stress and mobilized shear strength

The Case-III is considered for further examination of the development of shear stress and mobilized shear strength along the potential failure plane. Figure 3 shows the variation of shear stress along the failure plane with movement of excavated/eroded block. Shear stress for four displacements (115 mm, 245 mm, 380 mm and 500 mm) are shown. In order to explain the process, consider the shear stress on the potential failure plane for the block displacement of 115 mm. The maximum shear stress (50 kPa) is developed at 12.5 m from the vertical face of the cut. The shear stress between 0 to 12.5 m is less than 50 kPa (i.e. s_{up}) and greater than 10 kPa (i.e. s_{ur}). That means, 0-12.5 m of the shear band represents the post-peak softening zone where the reduction of shear strength is occurred because of plastic strain as Eq. 2, and the mobilized shear strength is in between the peak and residual shear strength of the soil. In the right side of the peak (i.e. distance greater than 12.5 m) the shear stress is again reduced with distance. For this displacement of the block (115 mm), the shear stress in the

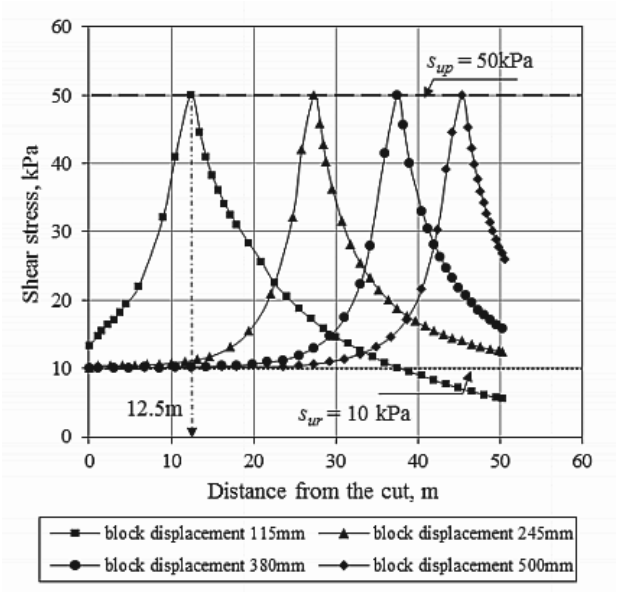

Figure 3. Shear stress along the potential failure plane

potential failure plane at a distance greater than 12.5 m is not increased to the peak, and therefore it represents the pre-peak behavior. At a very large distance, the shear stress is reduced to zero in Case-III as the ground surface is horizontal. The pattern of shear stress development for any other displacement of the block is similar as shown in Fig. 3. The location of the peak shear stress shifts to the right with increase in block displacement; that means a greater length of the potential failure plane is in post-peak stress-strain condition. For example, for 500 mm block movement the peak is occurred at 45.5 m and therefore 0-45.5 m is in post-peak condition with approximately 30 m in residual shear strength level. This process will be continued until the shear band propagation is ended for stable slopes as in Case-III. However, if the failure is occurred, as in Case-I and II, the large plastic shear strain will reduce the shear

strength of soil in the entire failure plane to the residual shear strength and global failure will occur.

Figure 4 shows the variation of shear stress at 4 different locations A, B, C and D (Fig. 1) which are located from the vertical face of the excavated/eroded block at horizontal distance of 3 m, 12.5 m, 25 m and 35 m, respectively. Consider the soil element B at 12.5 m distance. The shear stress in this element is increasing with movement of the excavated/eroded soil block. When the block is displaced by an amount of 115 mm, the shear stress in this element is reached to the peak shear strength of the soil (50 kPa). However, at this displacement of the block, the element A is almost at the residual shear strength. On the other hand, the elements C and D are still in the pre-peak state. That means the shear stress is gradually transferred to the soil elements in the right with displacement of the excavated/eroded soil block. For the soil element under the slope of the river bank there is an initial shear stress. With movement of the block the shear stress is increased from that initial value. However, the initial shear stress is less in the elements far from the river bank. Similar variation in shear stress and mobilized shear strength are obtained for Case-I and II.

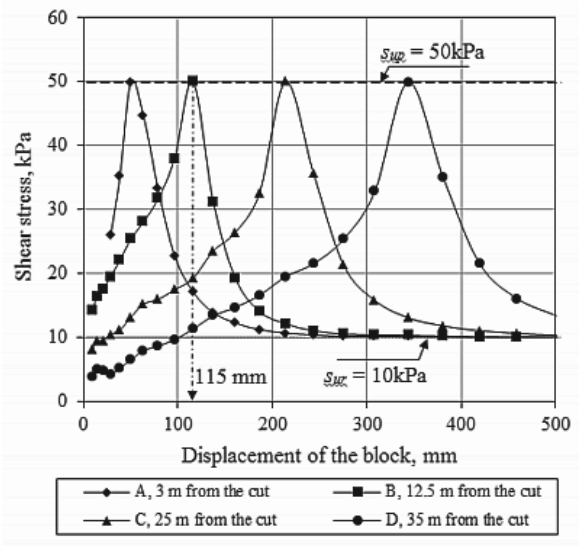

Figure 4. Variation of shear stress at four different locations from the cut

5. CONCLUSION

This paper presents a new numerical approach to model the initiation and propagation of shear band in upward progressive failure as encountered near the river banks. Toe erosion is considered as the triggering factor. Coupled Eulerian-Lagrangian (CEL) approach currently available in ABAQUS FE software is used for numerical analysis. Nonlinear strain softening behavior of sensitive clay is incorporated in this large deformation finite element analysis. Three cases are analyzed in this study. In Cases I and II global failure is occurred. However, in Case-III, although global failure is not occurred, the shear band propagation reduced the shear strength in the potential failure plane significantly over a large distance and the slope might be marginally stable for further loading.

6. ACKNOWLEDGEMENTS

The writers would like to acknowledge the financial support from Research & Development Corporation of Newfoundland and Labrador and C-CORE.

7. REFERENCES

Anderson L. and Jostad H.P. 2007. Numerical modeling of failure mechanisms in sensitive soft clays — application to offshore geohazards. Offshore Tech. Conf., Texas. Paper OTC 18650.

Bernander S. 2000. Progressive failure in long natural slopes: formation, potential extension and configuration of finished slides in strain-softening soils. Licentiate Thesis, Luleå University of Technology.

Bjerrum L. 1967. Progressive failure in slopes in overconsolidated plastic clay and clay shales. Terzaghi Lecture. J. of the Soil Mech. and Found. Div., ASCE 93(5), 3-49.

Carson M.A. 1979. On the retrogression of landslides in sensitive muddy sediments: Reply. Can. Geotech. J. 16(2), 431-444.

Cruden D.M. and Varnes D.J. 1996. Landslides types and processes. In Landslides investigation and mitigation. Special Report 247. Transportation Research Board, NRC. Edited by A.K. Turner and R.L. Schuster. National Academy Press, Washington, D.C., 37-75.

Dey R., Hawlader B., Phillips R. and Soga K. 2012. Effects of shear band propagation on submarine landslide. Proc. of the 22nd Int. Offshore and Polar Engineering Conf., Rhodes, Greece,766- 773.

Einav I. and Randolph M.F. 2005. Combining upper bound and strain path methods for evaluating penetration resistance. Int. J. Num. Methods Engineering63(14), 1991-2016.

Grondin G. and Demers D. 1996. The Saint-Liguori flakeslide: Characterization and remedial works. In Proc. of the 7th Int. Symposium on Landslides, Trondheim, Norway, 2, 743-748.

Gregersen O. 1981. The quick clay landslide in Rissa, Norway. In Proc. of the 10th Int. Conf. on Soil Mech. and Foundation Engineering, Stockholm, Sweden. NGI, Publication No. 135, 421-426.

Karlsrud K., Aas G. and Gregersen O. 1984. Can we predict landslide hazards in soft sensitive clays? Summary of Norwegian practice and experiences. In Proc. of the 4th Int. Symposium on Landslides, Toronto, Ont., 1, 107-130.

Leroueil S. 2001. Natural slopes and cuts: movement and failure mechanisms. Géotechnique 51 (3), 197-243.

Locat A., Leroueil S., Bernander S., Demers D., Locat J. and Ouehb L. 2008. Study of a lateral spread failure in an eastern Canada clay deposit in relation with progressive failure: the Saint-Barnabé-Nord slide. In Proc. of the 4th Canadian Conf. on Geohazards: From Causes to Management, Québec, Que., 89-96.

Locat A., Leroueil S., Bernander S., Demers D., Jostad H.P. and Ouehb L. 2011. Progressive failures in eastern Canadian and Scandinavian sensitive clays. Can. Geotech. J. 48 (11), 1696-1712.

NGI Report 2001. Effect of strain softening on stability analysis. Analysis of retrogressive sliding due to strain softening-Ormen Lange case study, Report No 521001 (10).

Odenstad S. 1951. The landslide at Sköttorp on the Lidan River, February 2, 1946. Royal Swedish Institute Proceedings 4, 1-38.

Quinn P., Diederichs M.S., Hutchinson D.J. and Rowe R.K. 2007. An exploration of the mechanics of retrogressive landslides in sensitive clay. In Proc. of the 60th Canadian Geotechnical Conf., Ottawa, Ontario, 721-727.

Quinn P. 2009. Large Landslides in Sensitive Clay in Eastern Canada and the Associated Hazard and Risk to Linear Infrastructure. Doctoral thesis, Queen's University.

Tavenas F., Flon P., Leroueil S. and Lebuis J. 1983. Remolding energy and risk of slide retrogression in sensitive clays. Proc. of the Symposium on Slopes on Soft Clays, Linköping, Sweden, SGI Report No. 17, 423-454.

Tavenas F. 1984. Landslides in Canadian sensitive clays — a state-of the-art. In Proc. of the 4th Int. Symposium on Landslides, Toronto, Ont., 1, 141-153.